Quench dynamics of the Kondo effect: Transport across an impurity coupled to interacting wires

Moallison F. Cavalcante [1,2] Rodrigo G. Pereira [3] and Maria C. O. Aguiar [1]

[1]*Departamento de Física, Universidade Federal de Minas Gerais, C. P. 702, 30123-970 Belo Horizonte, MG, Brazil*

[2]*Université Paris-Saclay, CNRS, Laboratoire de Physique des Solides, 91405 Orsay, France*

[3]*International Institute of Physics and Departamento de Física Teórica e Experimental, Universidade Federal do Rio Grande do Norte, 59072-970 Natal-RN, Brazil*

(Received 4 November 2022; accepted 24 January 2023; published 6 February 2023)

We study the real-time dynamics of the Kondo effect after a quantum quench in which a magnetic impurity is coupled to two metallic Hubbard chains. Using an effective field theory approach, we find that for noninteracting electrons the charge current across the impurity is given by a scaling function that involves the Kondo time. In the interacting case, we show that the Kondo time decreases with the strength of the repulsive interaction and the time dependence of the current reveals signatures of the Kondo effect in a Luttinger liquid. In addition, we verify that the relaxation of the impurity magnetization does not exhibit universal scaling behavior in the perturbative regime below the Kondo time. Our results highlight the role of nonequilibrium dynamics as a valuable tool in the study of quantum impurities in interacting systems.

DOI: 10.1103/PhysRevB.107.075110

I. INTRODUCTION

Quantum impurity problems in low-dimensional systems have been of great importance to the understanding of many-body systems for a long time [1]. The interaction between the impurity and the bulk degrees of freedom can be approached theoretically using well-established analytical approaches based on exact solutions [2,3], and boundary conformal field theory [4,5] and numerical methods such as the numerical renormalization group [6] and the density matrix renormalization group (DMRG) [7]. At the same time, a steady development of experimental techniques to control and probe synthetic quantum matter in quantum dots [8,9] and ultracold atoms [10–13] opens the possibility of testing many theoretical scenarios.

A currently active area of research is the study of the real-time dynamics of quantum many-body systems driven out of equilibrium [14,15]. A simple way of simulating the nonequilibrium dynamics in closed systems is by means of quantum quench protocols [15–18]. Consider a system described by a Hamiltonian $H(g)$, where g stands for a parameter or a set of parameters, and suppose that the system is initially prepared in the ground state $|\Psi_0\rangle$ of $H(g)$. A quantum quench is defined by a sudden (much faster than any other characteristic internal time scale) change $H \to H' = H(g')$, followed by the unitary evolution of the system under H'.

In this work, we investigate the formation of the Kondo effect [19] in the real-time dynamics following a quantum quench. In electronic systems, the Kondo effect arises when the spin of a localized magnetic impurity couples to conduction electrons via an antiferromagnetic exchange interaction with Kondo coupling $J_K > 0$. The hallmark of this effect is the emergence of an energy scale, $k_B T_K$, where k_B is the Boltzmann constant and T_K the Kondo temperature, which marks a crossover from weak coupling at temperatures $T \gg T_K$ to strong coupling at $T \ll T_K$. The crossover can be detected in various observables that behave as scaling functions of T/T_K. For instance, at high temperatures the impurity magnetic susceptibility exhibits a logarithmic scaling, $\chi_{\rm imp} \sim \ln(T_K/T)$, characteristic of the perturbative renormalization of the effective Kondo coupling. At $T \lesssim T_K$, perturbation theory in the Kondo coupling breaks down, and the low-temperature regime $T \ll T_K$ is described by the localized spin forming a singlet state with a conduction electron. In this regime, the impurity susceptibility shows a $(T/T_K)^2$ dependence governed by irrelevant perturbations to the strong-coupling fixed point [20]. In quantum wires with finite length L, the crossover can occur at zero temperature as a function of the ratio L/ξ_K, where $\xi_K = \hbar v_F/(k_B T_K)$ (with v_F the Fermi velocity) is the size of the Kondo cloud that surrounds and screens the localized spin [21–26]. The Kondo cloud was recently observed in a mesoscopic device [27]. By analogy and dimensional analysis, one can argue for the existence of a Kondo time $t_K = \hbar/(k_B T_K)$. In fact, the latter shows up in time-dependent response functions [28] and can be interpreted as the time scale for the formation of the Kondo cloud after the Kondo coupling is suddenly switched on. The analogy with the equilibrium Kondo effect has motivated the search for universal scaling behavior in the time evolution after quenches in quantum impurity models [29–45].

Our goal is to observe the emergence of the Kondo time scale within an analytical approach for a quench protocol that probes charge transport across a magnetic impurity. Similar protocols have been studied in the anisotropic Kondo model with noninteracting leads [32,33] and in junctions of Luttinger liquids far from equilibrium without the localized spin [46]. Here we study the isotropic Kondo model including interactions in the leads. The schematic setup is shown in Fig. 1. We consider two electronic chains held at different chemical potentials and coupled to a singly occupied quantum dot that

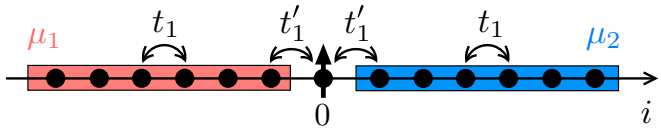

FIG. 1. Schematic setup for a quantum dot coupled to two semi-infinite chains. The hopping parameter in both chains is t_1. The quantum dot state at $i = 0$ has energy $\epsilon_d < 0$ and on-site electron-electron interaction $U_d > 0$. In the quench protocol, the single electron in the dot is initially polarized and the left and right chains are held at chemical potentials μ_1 and μ_2, respectively. At time $t = 0$, the dot is coupled to the chains with hopping parameter t_1'. After that, a charge current starts flowing across the dot, with a time dependence that reveals signatures of the Kondo effect.

acts as an $S = 1/2$ magnetic impurity. In the static problem in the linear response regime, this setup reveals signatures of the Kondo effect as the conductance across the dot scales with T/T_K, approaching the maximum value $2e^2/h$ for $T \to 0$ in the particle-hole symmetric case [1,47]. Here we shall look for scaling behavior as a function of the time ratio t/t_K after the chains are suddenly coupled to the impurity spin prepared in a polarized state. We consider both regimes of $t \ll t_K$ and $t \gg t_K$, governed by the weak- and strong-coupling fixed points of the Kondo model, respectively. Our results indicate that the charge current in the post-quench dynamics can be described by a scaling function of t/t_K in the case of noninteracting electrons in the leads. We then turn to interacting chains described by the Hubbard model and discuss how Luttinger liquid effects modify the exponents in the time dependence of the current as the system approaches the steady state. In this process, we also generalize previous results [48] for the real-time decay of the impurity magnetization, and show that the latter is not a universal function in the regime $t \ll t_K$.

This paper is organized as follows. In Sec. II we briefly review the derivation of the Kondo model for a quantum dot embedded between two tight-binding chains. We also introduce the quench protocol and discuss the time scales involved in the problem. In Sec. III we consider the current dynamics in the case of noninteracting electrons in the leads, identifying the scaling behavior as a function of t/t_K in both weak- and strong-coupling limits. In Sec. IV we discuss the effects of electron-electron interactions in the chains. Section V is devoted to the time dependence of the impurity magnetization. Our conclusions are summarized in Sec. VI. Finally, Appendix A contains the main bosonization formulas, and Appendix B focuses on the three-point function used in the perturbative calculations. Hereafter we set $\hbar = k_B = 1$.

II. MODEL AND QUENCH PROTOCOL

We investigate the post-quench dynamics of a quantum dot coupled to two semi-infinite chains, see Fig. 1. The system is described by the time-dependent Hamiltonian

$$H(t) = H_0 + H_U + H_d + \theta(t)H_{\rm coup}. \tag{1}$$

Here $H_0 = \sum_{\ell=1,2} H_\ell$ is the Hamiltonian for decoupled chains with

$$H_1 = -t_1 \sum_{i\leqslant -2} (c_i^\dagger c_{i+1} + \text{H.c.}), \tag{2}$$

$$H_2 = -t_1 \sum_{i\geqslant 1} (c_i^\dagger c_{i+1} + \text{H.c.}), \tag{3}$$

where t_1 is the hopping parameter in the chains and $c_i^\dagger = (c_{i\uparrow}^\dagger, c_{i\downarrow}^\dagger)$, with $c_{i\sigma}^\dagger$ the creation operator for an electron with spin σ at site i. The corresponding number operator is $n_{i\sigma} = c_{i\sigma}^\dagger c_{i\sigma}$. The second term in Eq. (1) accounts for electron-electron interactions in the chains:

$$H_U = U \sum_{i\neq 0} n_{i\uparrow} n_{i\downarrow}, \tag{4}$$

where $U \geqslant 0$ is the strength of the on-site repulsive interaction. The Hamiltonian for the dot (denoted as site $i = 0$) is given by

$$H_d = \epsilon_d n_0 + U_d n_{0\uparrow} n_{0\downarrow}, \tag{5}$$

where $n_0 = n_{0\uparrow} + n_{0\downarrow}$, ϵ_d is the energy of the localized state with respect to the Fermi level in the chains, and U_d is the local interaction. To favor a local moment at the quantum dot, we consider $\epsilon_d < 0$ and $U_d > 0$. The coupling term reads

$$H_{\rm coup} = -t_1' \, (c_{-1}^\dagger + c_1^\dagger) c_0 + \text{H.c.}, \tag{6}$$

where t_1' is the hybridization between the dot and the end sites of each chain.

The Kondo regime corresponds to $t_1' \ll -\epsilon_d, U_d$. In this case, we apply a Schrieffer-Wolff transformation to derive the effective Hamiltonian in the low-energy subspace with a single electron at the dot [19]. We obtain

$$H_{\rm eff}(t) = H_0 + H_U + \theta(t)(H_K + H_W), \tag{7}$$

where

$$H_K = J_K \mathbf{S}_0 \cdot (c_{-1}^\dagger + c_1^\dagger) \frac{\boldsymbol{\sigma}}{2} (c_{-1} + c_1),$$

$$H_W = W (c_{-1}^\dagger + c_1^\dagger)(c_{-1} + c_1). \tag{8}$$

Here H_K describes the Kondo interaction between conduction electrons in the symmetric channel and the impurity spin $\mathbf{S}_0 = c_0^\dagger (\boldsymbol{\sigma}/2) c_0$, with Kondo coupling

$$J_K = 2t_1'^2 \left(\frac{1}{-\epsilon_d} + \frac{1}{U_d + \epsilon_d} \right). \tag{9}$$

The strength of the potential scattering term H_W is

$$W = \frac{t_1'^2}{2} \left(\frac{1}{-\epsilon_d} - \frac{1}{U_d + \epsilon_d} \right). \tag{10}$$

Note that W vanishes in the particle-hole symmetric case $\epsilon_d = -U_d/2$.

We now focus on the model for noninteracting chains, $U = 0$, and analyze it in the continuum limit. We will discuss the interacting case in Sec. IV. We replace $c_{j\sigma}$ by a fermionic field operator $c_{\ell,\sigma}(x)$, where $c_{1,\sigma}(x)$ is defined for $x < 0$ and $c_{2,\sigma}(x)$ for $x > 0$. To describe the low-energy modes in the chains, we expand $c_{\ell,\sigma}(x)$ in terms of right (R) and left (L) movers:

$$c_{\ell,\sigma}(x) = e^{ik_F x} \psi_{R,\ell,\sigma}(x) + e^{-ik_F x} \psi_{L,\ell,\sigma}(x), \tag{11}$$

where k_F is the Fermi momentum, assumed to be the same for both chains at equilibrium. Particle-hole symmetry imposes half filling, $k_F = \pi/2$. For $t_1' = 0$, the open boundary condition $c_{\ell,\sigma}(0) = 0$ can be cast as a constraint on the chiral fermionic modes in each wire:

$$\psi_{L,\ell,\sigma}(x) = -\psi_{R,\ell,\sigma}(-x). \tag{12}$$

The above constraint allows us to work with a single chiral mode redefined in the domain $x \in \mathbb{R}$ [49]:

$$\begin{aligned}\psi_1^\dagger(x) &\equiv (\psi_{L,1,\uparrow}^\dagger(-x), \psi_{L,1,\downarrow}^\dagger(-x)),\\ \psi_2^\dagger(x) &\equiv (\psi_{R,2,\uparrow}^\dagger(x), \psi_{R,2,\downarrow}^\dagger(x)).\end{aligned} \tag{13}$$

In the continuum limit, the noninteracting Hamiltonian in the leads can be written as

$$H_0 = v_F \sum_\ell \int dx\, \psi_\ell^\dagger(-i\partial_x)\psi_\ell\,, \tag{14}$$

with Fermi velocity $v_F = 2t_1 \sin k_F$. For small t_1', we can treat the local interactions as perturbations to the weak-coupling fixed point $J_K = W = 0$. In terms of the fermionic fields, we have

$$H_K = \pi v_F \lambda_K \mathbf{S}_0 \cdot \sum_{\ell,\ell'} :\psi_\ell^\dagger(0)\frac{\boldsymbol{\sigma}}{2}\psi_{\ell'}(0):, \tag{15}$$

$$H_W = W' \sum_{\ell,\ell'} :\psi_\ell^\dagger(0)\psi_{\ell'}(0):, \tag{16}$$

where $\lambda_K = 4J_K \sin^2 k_F/(\pi v_F)$ is the dimensionless Kondo coupling, $W' = 4W \sin^2 k_F$, and :: denotes normal ordering.

In the static problem, the effective Kondo coupling at energy scale Λ obeys the renormalization group (RG) equation [5,19]

$$\frac{d}{dl}\lambda_K = \lambda_K^2 + \mathcal{O}\big(\lambda_K^3\big), \tag{17}$$

where $l = \ln(\Lambda_0/\Lambda)$ with $\Lambda_0 \sim t_1$ the bare cutoff. In contrast, the potential scattering parameter W' is strictly marginal. As a result, the low-energy physics is dominated by the flow of λ_K to strong coupling, in the form

$$\lambda_K^{\rm eff}(l) \approx \frac{\lambda_0}{1-\lambda_0 l}, \tag{18}$$

where $\lambda_0 = \lambda_K^{\rm eff}(0)$ is the bare coupling constant. In the lattice picture for the strong-coupling fixed point $\lambda_K \to \infty$, the impurity forms a singlet with an electron in the symmetric orbital associated with $(c_1^\dagger + c_{-1}^\dagger)/\sqrt{2}$ [22,23]. At low energies, this symmetric orbital is blocked by a binding energy of order $T_K \sim \Lambda_0 e^{-1/\lambda_0} \ll \Lambda_0$. This effect changes the boundary conditions for the symmetric channel, but electrons can move freely between the chains through the anti-symmetric orbital associated with $(c_1^\dagger - c_{-1}^\dagger)\sqrt{2}$. For $W' = 0$, the strong-coupling fixed point is characterized by the ideal conductance $G_0 = e^2/\pi$ (in unit of $\hbar = 1$). More generally, the conductance is lowered by the potential scattering term allowed in the case of broken particle-hole symmetry [22].

To study the post-quench dynamics of the model, we consider that for times $t < 0$ the system is prepared in the state

$$|\Psi_0\rangle = |\psi_0\rangle_1 \otimes |\uparrow\rangle \otimes |\psi_0\rangle_2, \tag{19}$$

where $|\psi_0\rangle_\ell$ for $\ell = 1, 2$ denote the ground states of the disconnected chains and $|\uparrow\rangle$ is the spin-polarized state of the impurity. For times $t > 0$, we switch on the Kondo interaction and the state evolves nontrivially as

$$|\Psi(t>0)\rangle = e^{-iH_{\rm eff}t}|\Psi_0\rangle. \tag{20}$$

By analogy with the static problem [19], we expect the infrared singularity associated with the Kondo effect to be cut off by the finite time after the impurity is coupled to the leads. Thus, the dynamics in the time regime $t \ll t_K$ must be governed by the weak-coupling fixed point and λ_K can be treated as a perturbative parameter. For times $t \sim t_K$, the dimensionless Kondo coupling must become of order one, implying that the perturbative expansion breaks down. For $t \gg t_K$, the dynamics is controlled by the strong-coupling fixed point. Besides the Kondo time scale, the low-energy theory may involve another important time scale, Λ_0^{-1}, related to the microscopic details of the lattice model in Eq. (1). Since our quench is instantaneous, the latter is the shortest time scale in the problem. The field theory results discussed in the following require $t \gg \Lambda_0^{-1}$, but we should still observe a crossover in the physical properties of the system between the intermediate-time regime $\Lambda_0^{-1} \ll t \ll t_K$ and the long-time regime $t \gg t_K$.

III. CHARGE TRANSPORT ACROSS THE IMPURITY

In this section we discuss the dynamics of the charge current after the impurity is coupled to the noninteracting chains with a small voltage bias. Unless otherwise stated, we assume particle-hole symmetry and set $W' = 0$.

A. Weak coupling

To study time-dependent transport, we consider different chemical potentials μ_ℓ in the chains. The Hamiltonian for $t > 0$ is modified by

$$H \to H + \sum_{\ell=1,2} \mu_\ell N_\ell, \tag{21}$$

where N_ℓ is the total number operator for electrons in chain ℓ. The chemical potential term in Eq. (21) can be traded for a time-dependent vector potential using the gauge transformation $\psi_\ell \to e^{-i\mu_\ell t}\psi_\ell$, at the price of introducing an explicit time dependence in H [46].

The current operator in the continuum limit is

$$\begin{aligned}\hat{j}(t) &= e\frac{d}{dt}(N_1 - N_2) = ie[H_K, N_1 - N_2],\\ &= ie\pi v_F \lambda_K [e^{ieVt}\mathbf{S}_0 \cdot \psi_2^\dagger(0)\boldsymbol{\sigma}\psi_1(0) - \text{H.c.}],\end{aligned} \tag{22}$$

where $V \equiv (\mu_2 - \mu_1)/e$ plays the role of a bias voltage. In the following we focus on the linear response regime and assume that eV is the smallest energy scale in the problem, therefore all our time-dependent transport results are limited by the time $t \ll t_V \equiv |eV|^{-1}$. The current at time $t > 0$ is given by

$$\begin{aligned}j(t) &= \langle\Psi(t)|\hat{j}(t)|\Psi(t)\rangle,\\ &= \langle T\,\hat{j}_I(t)\,\mathcal{U}_{\rm Kel}\rangle_0,\end{aligned} \tag{23}$$

where $\hat{j}_I(t) = e^{iH_0 t}\hat{j}(t)e^{-iH_0 t}$ is the current operator evolved in the interaction picture, H_0 is written in the continuum limit as in Eq. (14), and $\langle\,\rangle_0$ denotes the expectation value in $|\Psi_0\rangle$. Here T is the time-ordering operator in Keldysh contour γ and

$$\mathcal{U}_{\rm Kel} = \exp\left[-i\int_\gamma dt' H_{K,I}(t')\right] \tag{24}$$

is the time evolution operator in γ [50] involving the Kondo interaction $H_{K,I}(t) = e^{iH_0 t}H_K e^{-iH_0 t}$ with H_K given in Eq. (15).

In the time regime $t \ll t_K$, the Kondo coupling can be treated perturbatively. Expanding the exponential in Eq. (24) in powers of λ_K and rewriting $\int_\gamma = \int_{\gamma^+} + \int_{\gamma^-}$, with γ^- (γ^+) the time (anti-time)-ordered branch, we obtain a perturbative series for the current in Eq. (23). The lowest-order terms in this series are

$$j^{(2)}(t) = i\int_0^t dt' \langle [H_{K,I}(t'), \hat{j}_I(t)]\rangle_0, \tag{25}$$

$$j^{(3)}(t) = -\frac{1}{2}\int_0^t dt' dt'' [\langle \hat{j}_I(t) T H_{K,I}(t') H_{K,I}(t'')\rangle_0 + \text{H.c.} - 2\langle H_{K,I}(t')\hat{j}_I(t) H_{K,I}(t'')\rangle_0]. \tag{26}$$

Here $j^{(n)}(t)$ stands for the current at order λ_K^n, generated by expanding the time evolution operator to order λ_K^{n-1}. Note that the current operator in Eq. (22) already contains one factor of λ_K. Since $[H_0, \mathbf{S}_0] = 0$, the time dependence of the impurity spin correlators only comes from the time-ordering operator.

Calculating the correlator in Eq. (25), we obtain the linear-in-V contribution

$$j^{(2)}(t) = \frac{3ie^2 V\lambda_K^2}{8}\int_0^{\Lambda_0 t} du\,\frac{u}{[h(u)]^2} + \text{H.c.}, \tag{27}$$

where $h(u) = 1 + iu$. While the above integral can be computed analytically for arbitrary times, we are mostly interested in the regime $\Lambda_0 t \gg 1$. In this case, the leading term in the current behaves as

$$j^{(2)}(t) \approx \frac{3\pi^2 j_0}{8}\lambda_K^2\left[1 - \frac{4}{\pi\Lambda_0 t} + \mathcal{O}(t^{-3})\right], \tag{28}$$

where $j_0 = e^2V/\pi$ is the current for an ideal conductance. This result is the same as that for the transport across a nonmagnetic impurity [46]. As it stands, this result suggests that the current would approach a finite value corresponding to a small conductance of order λ_K^2.

To capture the Kondo effect, we need to include the contribution to the current at order λ_K^3. Given the initial state in Eq. (19) and the current operator in Eq. (22), the only impurity correlator that contributes to the current in Eq. (26) is

$$\left\langle T S_0^a(t) S_0^b(t') S_0^c(t'')\right\rangle_0 = \epsilon^{abc}\frac{i}{8}\epsilon(t,t',t''), \tag{29}$$

where ϵ^{abc} is the Levi-Civita symbol and $\epsilon(t,t',t'') = 1$ if $t > t' > t''$ and is completely antisymmetric under the exchange of t, t', t''. As for the conduction electrons, the nonzero correlators involve, for instance,

$$\langle T\psi_{1\downarrow}^\dagger(t)\psi_{2\uparrow}(t)\psi_{1\uparrow}^\dagger(t')\psi_{1\downarrow}(t')\psi_{2\uparrow}^\dagger(t'')\psi_{1\uparrow}(t'')\rangle_0, \tag{30}$$

$$\langle T\psi_{1\downarrow}^\dagger(t)\psi_{2\uparrow}(t)\psi_{2\uparrow}^\dagger(t')\psi_{1\downarrow}(t')[\rho_{1s}(t'') + \rho_{2s}(t'')]\rangle_0, \tag{31}$$

where $\rho_{\ell s} = (\rho_{\ell\uparrow} - \rho_{\ell\downarrow})/\sqrt{2}$ is defined in terms of $\rho_{\ell\sigma} =: \psi_{\ell\sigma}^\dagger\psi_{\ell\sigma}$: and all the fields act at $x = 0$. After integrating over t'' in Eq. (26), we obtain to linear order in V

$$j^{(3)}(t) = \frac{ie^2V\lambda_K^3}{4}\int_0^{\Lambda_0 t} du\,\frac{u\ln h(u)}{[h(u)]^2}\left\{1 - \frac{2[h(u)]^2}{u(u-2i)}\right\} + \text{H.c.} + \cdots, \tag{32}$$

where we drop terms that decay as $(\Lambda_0 t)^{-1}$ or faster for $\Lambda_0 t \gg 1$. This approximation is equivalent to taking the scaling limit of the Kondo model, $\Lambda_0 \to \infty$, $J_K \to 0$, with T_K fixed.

Evaluating the integral in Eq. (32) and combining the result with the leading contribution from Eq. (28), we obtain

$$j(t) \approx \frac{3\pi^2 j_0}{8}\lambda_K^2[1 + 2\lambda_K\ln(\Lambda_0 t)] + \mathcal{O}\big(\lambda_K^4\big). \tag{33}$$

In this perturbative regime, the time dependence of the current can be cast in the form $j(t) = j[\lambda_K^{\rm eff}(t)]$, where $j[\lambda_K] = \frac{3\pi^2 j_0}{8}\lambda_K^2$ and

$$\lambda_K^{\rm eff}(t) = \lambda_K + \lambda_K^2\ln(\Lambda_0 t) + \cdots \tag{34}$$

is the effective Kondo coupling at time scale t. This result confirms our expectation that the weak-coupling expansion should break down at long times, since the effective Kondo coupling diverges for $t \to \infty$. From Eq. (34), we can define the Kondo time by the condition $\lambda_K^{\rm eff}(t_K) \sim 1$ with bare coupling $\lambda_K = \lambda_0 \ll 1$. This condition gives $t_K \sim \Lambda_0^{-1}e^{1/\lambda_0} \gg \Lambda_0^{-1}$, as expected from the relation $t_K \sim 1/T_K$. From Eq. (18), we then have $\lambda_K^{\rm eff}(t) \approx [\ln(t_K/t)]^{-1}$ for $\Lambda_0^{-1} \ll t \ll t_K$, and we obtain

$$j(t) \approx \frac{3\pi^2}{8}\frac{j_0}{\ln^2(t_K/t)}. \tag{35}$$

This result was obtained in Ref. [33] based on poor man scaling's arguments. Here we have explicitly verified the scaling of the effective Kondo coupling by computing the third-order contribution to the time-dependent current.

The scattering potential term in Eq. (15) contributes to the current at order $(W')^2$ [46]. Since this term does not renormalize, the result in Eq. (33) is simply modified by a constant term. Similarly to the low-energy limit of the Kondo problem in the static case, the long-time limit of our dynamical problem is governed by the flow of λ_K to strong coupling. We will address this limit in the next subsection.

B. Strong coupling

In the limit $t \gg t_K$, the effective Kondo coupling diverges. The impurity spin is completely screened and removed from the low-energy theory. In the particle-hole symmetric case, $W' = 0$, the scattering phase shift associated with the Kondo effect in the symmetric channel [1,47] modifies the boundary conditions at the origin to

$$\psi_{L,2,\sigma}(0) = \psi_{R,1,\sigma}(0), \qquad \psi_{R,2,\sigma}(0) = \psi_{L,1,\sigma}(0). \tag{36}$$

Thus, the fixed-point Hamiltonian describes a single wire with perfect transmission at the origin:

$$H_{\rm sc} = v_F\int dx\,[\psi_R^\dagger(-i\partial_x)\psi_R + \psi_L^\dagger(i\partial_x)\psi_L]. \tag{37}$$

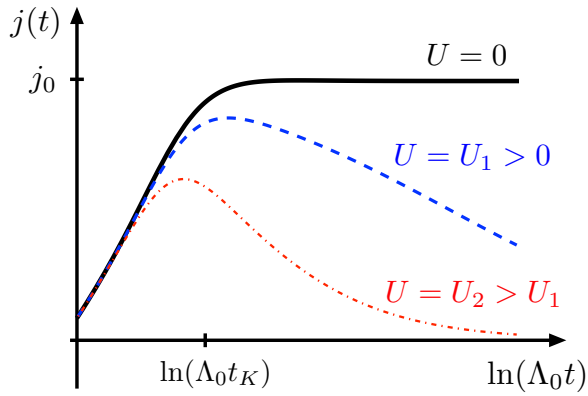

FIG. 2. Schematic time dependence of the current across the impurity spin after the quantum quench. Here $j_0 = G_0 V$ is the current for ideal conductance $G_0 = e^2/\pi$. The solid line represents the case of noninteracting electrons in the chains. In the time interval $\Lambda_0^{-1} \ll t \ll t_K$, described by the weak-coupling fixed point of the Kondo model, the current increases logarithmically with time, see Eq. (33). The long-time regime $t \gg t_K$ is described by the strong-coupling fixed point, see Eq. (39). The dashed and dot dashed lines represent the behavior for two different values of the repulsive electron-electron interaction in the leads, in which case the current vanishes as $\sim t^{1-K_c^{-1}}$ at long times [see Eq. (53) and Sec. IV C].

As a consequence, for sufficiently long times the current must approach the ideal conductance limit, $j(t \gg t_K) \to j_0$.

To analyze the long-time behavior, we can perturb the strong-coupling fixed point by its leading irrelevant operator. Since the impurity is screened, its spin operator does not appear in the low-energy effective Hamiltonian. According to local Fermi liquid theory [1,20], the leading irrelevant operator that respects SU(2) symmetry is

$$\delta H = g : \mathbf{J}^2(0) :, \tag{38}$$

where $\boldsymbol{J}(0) = \psi^\dagger(0)\frac{\sigma}{2}\psi(0)$ is the spin density at the origin and $g \sim 1/T_K \sim t_K$ is the coupling constant. The operator in Eq. (38) has scaling dimension equal to two; like any boundary operators with dimension greater than one, g is irrelevant in the RG sense. Considering the application of a small voltage V around the origin [51] and calculating the current at long times by perturbation theory to order g^2, we obtain

$$j(t) \approx j_0\left[1 - \left(\frac{t_K}{t}\right)^2\right]. \tag{39}$$

Thus, in the long-time regime the Kondo time t_K can be extracted from the coefficient of the $1/t^2$ term, which is absent in the intermediate-time regime, see Eq. (28). We recall that we always consider the time range $t \ll t_V = |eV|^{-1}$. At finite bias, the current would be influenced by oscillating terms with frequency eV (see, e.g., Ref. [33]).

The results in Eqs. (33) and (39) are illustrated in Fig. 2. They are analogous to the behavior of static properties of Kondo systems at finite temperature, such as the impurity susceptibility $\chi_{\rm imp}(T)$ [19], with the correspondence $T \leftrightarrow t^{-1}$. This correspondence reveals that, in the post-quench dynamics, time essentially acts as the inverse of an energy scale and the dynamics is effectively controlled by the RG flow from weak to strong coupling. At intermediate times, $t \sim t_K$, the problem becomes nonperturbative and we are not able to derive analytical expressions. However, since the Kondo effect is characterized by a crossover with a single emergent energy scale T_K, in general we expect a smooth function $j(t/t_K)$ connecting the asymptotic behavior in Eqs. (33) and (39).

For a system without particle-hole symmetry, we need to take into account an additional perturbation corresponding to a local potential barrier:

$$H_{\rm sc} \to H_{\rm sc} + \mathcal{W} : [\psi_R^\dagger(0) + \psi_L^\dagger(0)][\psi_R(0) + \psi_L(0)] :, \tag{40}$$

where $\mathcal{W}$ is the strength of the scattering potential. For noninteracting electrons, this term is a marginal perturbation. As a result, the constant value of the current at long times is reduced by a correction of order $\mathcal{W}^2$, but the time dependence is qualitatively the same as for $\mathcal{W} = 0$.

IV. LUTTINGER LIQUID EFFECTS

In this section we discuss how electron-electron interaction in the chains affect the Kondo effect in the post-quench dynamics. In this case, our model describes two semi-infinite Hubbard chains prepared in the ground state of $H_0 + H_U$ and suddenly coupled to a polarized impurity spin.

A. Low-energy Hamiltonian

The low-energy excitations in the chains are described by the Luttinger model [51,52]. Starting from $t_1' = 0$ (see Fig. 1), we take the continuum limit and write the interaction in terms of the chiral fermionic fields. The low-energy effective Hamiltonian for each chain reads

$$\begin{aligned} H_\ell^{\rm int} = \int dx \Big\{ & v_F \psi_\ell^\dagger(-i\partial_x)\psi_\ell \\ & + U \sum_\sigma : \psi_{\ell,\sigma}^\dagger(x)\psi_{\ell,-\sigma}^\dagger(-x)\psi_{\ell,\sigma}(-x)\psi_{\ell,-\sigma}(x) : \\ & + U \sum_\sigma \rho_{\ell,\sigma}(x)[\rho_{\ell,-\sigma}(x) + \rho_{\ell,-\sigma}(-x)] \Big\}, \end{aligned} \tag{41}$$

where we used the constraint in Eq. (12). Here we have omitted the Umklapp term, which oscillates in space for $k_F \neq \pi/2$ [51]. At halffilling, $k_F = \pi/2$, the Umklapp term becomes a relevant perturbation that drives the system to a Mott-insulating phase for arbitrarily small $U > 0$. For this reason, in the interacting case we stay away from halffilling, which entails breaking particle-hole symmetry.

We can diagonalize the interacting Hamiltonian in Eq. (41) using Abelian bosonization [51,52]. For open boundary conditions, the fermionic field operator assumes the form [49]

$$\psi_\ell(x) \sim \frac{1}{\sqrt{2\pi\alpha}} \begin{pmatrix} F_{\ell\uparrow} e^{-i\sqrt{\frac{\pi}{2}}[\phi_{\ell,c}(x) + \phi_{\ell,s}(x)]} \\ F_{\ell\downarrow} e^{-i\sqrt{\frac{\pi}{2}}[\phi_{\ell,c}(x) - \phi_{\ell,s}(x)]} \end{pmatrix}, \tag{42}$$

where $\alpha \sim v_F/\Lambda_0$ is a short-distance cutoff, $F_{\ell\sigma}$ are Klein factors that ensure the anticommutation relations between electrons with opposite spin, and $\phi_{\ell,\lambda}(x)$ with $\lambda = c, s$ are chiral bosonic fields associated with charge and spin collective

modes, which obey

$$[\phi_{\ell,\lambda}(x), \phi_{\ell',\lambda'}(y)] = i\delta_{\ell\ell'}\delta_{\lambda\lambda'}\mathrm{sgn}(x-y). \tag{43}$$

In terms of bosonic annihilation operators $\eta_{\ell,\lambda,q}$ with momentum $q > 0$, the fields $\phi_{\ell,\lambda}(x)$ are given by

$$\phi_{\ell,\lambda}(x) = \sum_{q>0} \frac{e^{-\frac{\alpha}{2}q}}{\sqrt{qL}}[z_{\lambda q}(x)\eta_{\ell,\lambda,q} + z^*_{\lambda q}(x)\eta^\dagger_{\ell,\lambda,q}], \tag{44}$$

where L is the length of the open chain, $z_{\lambda q}(x) = (1/\sqrt{K_\lambda})\cos(qx) + i\sqrt{K_\lambda}\sin(qx)$, and K_c and K_s are the Luttinger parameters in the charge and spin sectors, respectively. For the Hubbard model with $U \geqslant 0$, we have $1/2 < K_c \leqslant 1$, with $K_c = 1$ corresponding to the free-fermion point. In the spin sector, the SU(2) spin-rotation symmetry fixes $K_s = 1$ [51,52].

The bosonized Hamiltonian for an interacting chain in Eq. (41) can be written as

$$H^{\mathrm{int}}_\ell = H^{\mathrm{LL}}_\ell + H^{\mathrm{bs}}_\ell, \tag{45}$$

where the first term describes a Luttinger liquid with open boundary conditions:

$$H^{\mathrm{LL}}_\ell = \sum_{\lambda=c,s}\sum_{q>0} v_\lambda q\, \eta^\dagger_{\ell,\lambda,q}\eta_{\ell,\lambda,q}. \tag{46}$$

Here v_c and v_s are the velocities of the charge and spin bosonic modes, respectively. While bosonization yields perturbative expressions for the velocities and Luttinger parameters for small U, the Luttinger liquid Hamiltonian holds in general as the low-energy fixed point for any metallic (gapless) system in one dimension [53]. The second term in Eq. (45) corresponds to the backscattering operator in the second line of Eq. (41). For the SU(2)-symmetric model with $U > 0$, this term is known to be marginally irrelevant [51,52]. In the following we neglect the effects of the backscattering term and approximate $H^{\mathrm{int}}_\ell \approx H^{\mathrm{LL}}_\ell$.

We can now couple the quantum dot in the Kondo regime to the Luttinger liquid leads [49,54–56]. We rewrite the Kondo interaction as

$$H^{\mathrm{int}}_K = \pi v_F \lambda_K \mathbf{S}_0 \cdot \sum_\ell : \psi^\dagger_\ell(0)\frac{\boldsymbol{\sigma}}{2}\psi_\ell(0) : + \pi v_F \Gamma_K \mathbf{S}_0 \cdot \left[: \psi^\dagger_1(0)\frac{\boldsymbol{\sigma}}{2}\psi_2(0) + \mathrm{H.c.}\right] : . \tag{47}$$

In addition, we now distinguish between the dimensionless Kondo coupling within the same wire, λ_K, and the coupling Γ_K associated with tunneling across the impurity because these operators acquire different scaling dimensions in the interacting case. The bosonization of the Kondo interaction can be obtained from Eq. (42). Close to the weak-coupling fixed point, the couplings $\lambda_K, \Gamma_K \ll 1$ obey the RG equations [49]

$$\frac{d}{dl}\lambda_K = \frac{1}{2}\left(\lambda_K^2 + \Gamma_K^2\right), \tag{48}$$

$$\frac{d}{dl}\Gamma_K = \frac{1}{2}\left(1 - K_c^{-1}\right)\Gamma_K + \lambda_K\Gamma_K. \tag{49}$$

For a repulsive interaction, $K_c < 1$, the coupling Γ_K initially decreases under the RG flow. However, since $\lambda_K > 0$ always increases, the second term in Eq. (49) ultimately drives Γ_K to strong coupling as well.

The perturbative RG equations indicate that the low-energy limit of the Kondo model with interacting chains is still described by a strong-coupling fixed point where the impurity spin is screened by the conduction electrons. However, away from halffilling, the scattering potential term in Eq. (40) is allowed by symmetry as a perturbation to the fixed point with ideal conductance. Even if we assume a small $\mathcal{W}$, the backscattering part of this term flows to strong coupling as $d\mathcal{W}/dl = (1 - K_c)\mathcal{W}/2$. As a consequence, the effective height of the potential barrier diverges. At low energies, we recover two decoupled Luttinger liquids with open boundary conditions, with one electron in the symmetric channel having been removed to form a singlet with the impurity spin. This picture for the Kondo effect in a Luttinger liquid suggests that the time dependence of the current in our quench protocol can be strongly affected by interactions, as we shall discuss in the following.

B. Weak coupling

We now turn to the post-quench dynamics for interacting electrons. As discussed in Sec. II, we assume that the system has been prepared in the ground state of the Hamiltonian for decoupled chains. Within the low-energy theory, the ground state $|\psi_0\rangle_\ell$ of the Hubbard chains corresponds to the vacuum of charge and spin bosons, $\eta_{\ell,\lambda,q}|\psi_0\rangle_\ell = 0$ for $\lambda = c, s$ and all $q > 0$.

Once again, we start by calculating the time-dependent current using perturbation theory in the Kondo coupling. The first terms in the series expansion of $j(t)$ are still given by Eqs. (25) and (26), but we now use the bosonized expressions for the current operator and the Kondo interaction given in Appendix A. The bias voltage is implemented as a time-dependent shift of the charge bosons, $\phi_{\ell,c} \to \phi_{\ell,c} + \sqrt{\frac{2}{\pi}}\mu_\ell t$. The correlators involve exponentials of the bosonic fields, see Eq. (42). At order λ_K^2, we need two-point functions of the form [51,52]

$$\left\langle e^{ia\phi_{\ell,\lambda}(t)} e^{-ib\phi_{\ell',\lambda'}(t')}\right\rangle_0 = \frac{\delta_{ab}\delta_{\ell\ell'}\delta_{\lambda\lambda'}}{[1 + i\Lambda_0(t-t')]^{a^2/\pi K_\lambda}}, \tag{50}$$

where $a \in \mathbb{R}$. At order λ_K^3, correlators such as the one in Eq. (30) can be calculated using Eq. (50). On the other hand, the bosonized form of the correlator in Eq. (31) is proportional to

$$\left\langle T e^{-i\sqrt{\pi}[\phi_s^+(t) - \phi_c^-(t)]} e^{i\sqrt{\pi}[\phi_s^+(t') - \phi_c^-(t')]}\partial_x\phi_s^+(t'')\right\rangle_0, \tag{51}$$

where we define the symmetric and antisymmetric combinations

$$\phi^\pm_\lambda(x) = \frac{\phi_{1,\lambda}(x) \pm \phi_{2,\lambda}(x)}{\sqrt{2}}, \tag{52}$$

which obey $[\phi^\sigma_\lambda(x), \phi^{\sigma'}_{\lambda'}(y)] = i\delta_{\sigma\sigma'}\delta_{\lambda\lambda'}\mathrm{sgn}(x-y)$. To calculate the spin part of this correlator, we need to contract $\partial_x\phi^+_s$ with the exponentials using Wick's theorem as explained in Appendix B. We have checked that our result agrees with the correlator obtained in fermionic language in the noninteracting limit $K_c \to 1$.

After calculating the correlators, we find that the leading contributions to the current in the interacting case are obtained by replacing $[h(u)]^2 \to [h(u)]^{1+K_c^{-1}}$ in Eqs. (27) and (32). The

Luttinger parameter K_c also appears in the subleading contributions omitted in Eq. (32). For the time regime $\Lambda_0 t \gg 1$, we can calculate the integrals analytically to obtain

$$j(t) = \frac{3\pi j_0}{4} \frac{\sin(\pi\nu/2)\Gamma_K^2}{\nu(\Lambda_0 t)^\nu}[1 + 2\lambda_K \ln(\tilde{\Lambda}_0 t)] + \mathcal{O}\big(\Gamma_K^4\big), \tag{53}$$

where $\nu = K_c^{-1} - 1$, $\tilde{\Lambda}_0 = \Lambda_0 \exp[\frac{1}{\nu} - \frac{\pi}{2}\cot(\frac{\pi\nu}{2})]$ and we assumed $\alpha\Lambda_0 \approx v_F$. It is easy to verify that Eq. (53) reduces to Eq. (33) if we take $\Gamma_K = \lambda_K$ and $K_c \to 1$. In the above expression we can recognize the competing effects in the intertwined RG equations (48) and (49). At second order, we find a power-law decrease in the effective tunneling amplitude Γ_K, but at third order there is a logarithmic enhancement due to the coupling between Γ_K and λ_K.

We can rewrite Eq. (53) in terms of a renormalized coupling as

$$j(t) = \frac{3\pi j_0}{4} \frac{\sin(\pi\nu/2)}{\nu} \big[\Gamma_K^{\rm eff}(t)\big]^2, \tag{54}$$

where

$$\Gamma_K^{\rm eff}(t) \approx \frac{1}{(\Lambda_0 t)^{\nu/2}} \frac{\Gamma_K}{1 - \lambda_K \ln(\tilde{\Lambda}_0 t)}. \tag{55}$$

Besides two independent Kondo couplings, Γ_K and λ_K, the expression in Eq. (55) involves the high-energy cutoff in the power-law decaying factor. The interactions in the wires destroy the universal scaling of the Kondo problem in the sense that it is no longer possible to write the current, or any other physical quantity, as a function of t/t_K only. Nevertheless, it is instructive to analyze the weakly interacting limit $U \ll t_1$, where we have $K_c \approx 1 - U/(\pi v_F)$ [51]. In this case, λ_K and Γ_K start off approximately equal and flow together to strong coupling. Perturbation theory breaks down when $\lambda_K \ln(\tilde{\Lambda}_0 t) \sim 1$, which gives an estimate for the time scale

$$\tilde{t}_K \sim t_K \left(1 - \frac{\pi U}{12 v_F}\right), \tag{56}$$

where $t_K = \Lambda_0^{-1} e^{1/\lambda_K}$ is the Kondo time in the noninteracting case and we have expanded the renormalized cutoff to first order in U. In principle, at higher orders the dimensionless Kondo coupling λ_K may pick up a U dependence as well, but in the weakly interacting limit this dependence can be ignored in Eq. (56). According to Eq. (56), the time $\tilde{t}_K$ decreases with the interaction in the wires; in other words, repulsive interactions in the wires speed up the formation of Kondo singlet state. The same conclusion was reached numerically in Ref. [48].

Since particle-hole symmetry is broken away from half-filling, we also need to consider the perturbation in Eq. (16). In bosonized form, the intrawire part of this potential scattering term is proportional to $\partial_x \phi_c^+(0)$ and produces a constant contribution to the current. On the other hand, the tunneling term is proportional to $\cos[\sqrt{\pi}\phi_c^-(0) + eVt]\cos[\sqrt{\pi}\phi_s^-(0)]$, yielding a contribution that decays with time as $1/t^\nu$, as expected from the scaling dimension of this operator.

C. Strong coupling

We now turn to the long-time regime $t \gg \tilde{t}_K$. As discussed in Sec. III B, this regime is governed by perturbations to the strong-coupling fixed point. The main difference from the noninteracting case is that the potential scattering term in Eq. (40) now has scaling dimension $(1 + K_c)/2$ and becomes relevant for repulsive interactions. In this case, the stable low-energy fixed point of the Kondo model consists of two decoupled semi-infinite Luttinger liquids [49]. Since this fixed point has vanishing conductance, we expect $j(t \to \infty) = 0$. The leading perturbation is the irrelevant tunneling between the wires, equivalent to the interwire term in Eq. (16). Thus, we conclude that, after the impurity spin has been effectively screened, the current goes to zero as $j(t) \sim 1/t^\nu$. This behavior is represented by the dashed and dot dashed lines in Fig. 2.

V. IMPURITY MAGNETIZATION

In this section we consider the time evolution of the impurity magnetization after the quantum quench. The purpose is to connect with the results of Ref. [48], where second-order perturbation theory in the Kondo coupling was used to analyze numerical data from time-dependent DMRG. Here we extend this calculation to third order and contrast the behavior of impurity magnetization with that of the charge current discussed in Sec. III.

We now consider the simpler setup in which the impurity is coupled at the edge of a single chain, say $\ell = 2$ in Fig. 1. In this case the Kondo interaction is

$$H_K' = J_K \mathbf{S}_0 \cdot c_1^\dagger \frac{\boldsymbol{\sigma}}{2} c_1, \tag{57}$$

where J_K is still given by Eq. (9). To obtain the low-energy effective Hamiltonian, we proceed as in Sec. IV. Using the bosonization mapping and neglecting the irrelevant backscattering term in the interacting case, we obtain the effective Hamiltonian

$$H' = H^{\rm LL} + \pi v_s \lambda_K \bigg[S_0^+ \frac{e^{-i\sqrt{2\pi}\phi_s(0)}}{2\pi\alpha} + S_0^- \frac{e^{i\sqrt{2\pi}\phi_s(0)}}{2\pi\alpha} - S_0^z \frac{1}{\sqrt{2\pi}} \partial_x \phi_s(0) \bigg], \tag{58}$$

where we drop the index ℓ in the fields for a single chain. Remarkably, in the above Hamiltonian the Kondo interaction only involves the spin boson ϕ_s. This is a result of spin-charge separation in the geometry with an impurity coupled to the edge of a single wire [25]. Thus, unlike the case of an impurity embedded between two wires discussed in the previous sections, in this case the charge sector remains free and, as a consequence, the Luttinger parameter K_c does not appear in correlators for the electron spin density.

The impurity magnetization is given by

$$m_0(t) = \langle \Psi(t) | S_0^z | \Psi(t) \rangle. \tag{59}$$

We can apply perturbation theory in λ_K to obtain an expression for $m_0(t)$ valid in the regime $t \ll t_K$. Alternatively, we can employ a description similar to that used in the calculation

of the charge current and consider the quantity [cf. Eq. (22)]

$$\hat{j}_s^z = \frac{d}{dt}S^z = \pi v_s \lambda_K : \psi^\dagger(0)(\mathbf{S}_0 \times \boldsymbol{\sigma})_z \psi(0) :, \tag{60}$$

where S^z is the z component of the total spin operator for electrons in the wire. The operator in Eq. (60) represents the spin current that flows to the wire after the quench. In terms of the bosonic fields, the spin current reads

$$\hat{j}_s^z = i\frac{v_s\lambda_K}{2\alpha}\left[S_0^+ e^{-i\sqrt{2\pi}\phi_s(0)} - S_0^- e^{i\sqrt{2\pi}\phi_s(0)}\right]. \tag{61}$$

Since the entire system conserves spin, the impurity magnetization is related to the spin current for $t > 0$ by

$$j_s^z(t) + \frac{d}{dt}m_0(t) = 0, \tag{62}$$

where $j_s^z(t) = \langle\Psi(t)|\hat{j}_s^z|\Psi(t)\rangle$. This continuity equation allows us to obtain $m_0(t)$ by integrating $j_s^z(t)$ with the initial condition $m_0(0) = 1/2$.

We can now calculate $j_s^z(t)$ by perturbation theory in λ_K. The expansion is analogous to Eqs. (25) and (26). At order λ_K^2, we find that $j_s^z(t)$ decays as $1/t$ for $\Lambda_0 t \gg 1$. Integrating this leading contribution in time according to Eq. (62), we recover the logarithmic relaxation of the impurity magnetization observed in Ref. [48]. Going further and computing the third-order contribution, we obtain

$$j_s^z(t) = \frac{\lambda_K^2}{2t}[1 + 2\lambda_K \ln(\Lambda_0 t)] + \mathcal{O}\left(\lambda_K^4\right), \tag{63}$$

where we drop a subleading contribution that decays as $1/t^2$ in the regime $\Lambda_0 t \gg 1$. Thus, the spin current can be cast in the form $j_s^z(t) = [\lambda_K^{\text{eff}}(t)]^2/(2t)$ with $\lambda_K^{\text{eff}}(t)$ given in Eq. (34). On the other hand, using Eq. (62), we find that the impurity magnetization is given by

$$m_0(t) = \frac{1}{2} - \frac{\lambda_K^2}{2}\ln(\Lambda_0 t)[1 + \lambda_K \ln(\Lambda_0 t)] + \mathcal{O}\left(\lambda_K^4\right). \tag{64}$$

We note that $m_0(t)$ is not a function of the effective Kondo coupling and, consequently, not a function of t/t_K. In hindsight, this conclusion could have been anticipated by noting that the second-order term in Eq. (64) contains an explicit logarithmic dependence on the high-energy cutoff Λ_0 which is not related to the Kondo effect. We can further interpret this result using a simple scaling argument. The continuity equation implies that the current associated with any dimensionless conserved charge has dimensions of energy (or inverse time). For the charge current obtained in Eq. (33), the factor with dimensions of energy stems from the voltage bias eV that drives the current. In this case, the leading time dependence in the scaling limit enters in the renormalization of the dimensionless Kondo coupling. By contrast, the spin current in Eq. (63) is injected into the chain due to the relaxation of the impurity spin in the absence of perturbations such as a spin chemical potential bias. As a result of the scale invariance of the unperturbed system, the dimension contained in $j_s^z(t)$ appears as an explicit time dependence in the factor of $1/t$. This factor diverges for $t \to 0$, which implies that the integral of the spin current over time must include the short-time cutoff Λ_0^{-1}. This effect accounts for the additional cutoff dependence in the result of Eq. (64).

Finally, we note that Eq. (64) also describes the impurity magnetization in the embedded geometry of Fig. 1 for $U = 0$ since in this case we can rewritte the Kondo Hamiltonian only in terms of a single noninteracting channel ψ_+, where $\psi_\pm = (\psi_1 \pm \psi_2)/\sqrt{2}$ [22]. In the interacting case, the expression for $m_0(t)$ in the embedded geometry contains a contribution that decays as $1/t^\nu$ in order Γ_K^2 [48].

VI. CONCLUSION

We studied a quantum quench in which a magnetic impurity is suddenly coupled to the boundary of open chains. We focused on the real-time post-quench dynamics of two observables, the tunneling current across the impurity, and the impurity magnetization. For noninteracting electrons, we found that the time-dependent current is a scaling function of the ratio t/t_K. The regimes $t \ll t_K$ and $t \gg t_K$ are governed by the weak- and strong-coupling fixed points of the Kondo model, respectively. For interacting chains, the current at intermediate times exhibits a power-law dependence characteristic of Luttinger liquids physics and a logarithmic enhancement associated with the Kondo effect. Analyzing the weakly interacting case, we found that repulsive interactions decrease the Kondo time scale and favor the formation of the Kondo cloud, in accordance with previous numerical results [48]. Concerning the impurity magnetization, we concluded that the latter is not a function of the renormalized Kondo coupling in the regime $t \ll t_K$ because the perturbative result contains an explicit dependence on the short-time cutoff Λ_0^{-1} which is not related to the Kondo effect.

Our results emphasize the importance of identifying suitable physical properties when searching for Kondo physics in the real-time evolution. The scaling limit requires $t_K \gg \Lambda_0^{-1}$, making it challenging to observe the crossover from short to long times in currently available numerical simulations. Some advantage may be gained by considering time-dependent spin transport in the spin chain version of the Kondo model [57–59]. In this case, the charge degree of freedom is gapped out, and the model can be realized in the Mott-insulating phase of bosonic atoms in deep optical lattices. An important difference is that a magnetic impurity embedded between two Heisenberg spin chains gives rise to the two-channel Kondo effect, with a non-Fermi-liquid fixed point that may be manifested in the long-time post-quench dynamics. We leave this problem as a possible direction for future work.

ACKNOWLEDGMENTS

This work is supported by Fundação de Apoio à Pesquisa do Estado de Minas Gerais, Conselho Nacional de Desenvolvimento Científico e Tecnológico (in particular through INCT-IQ 465469/2014-0), and Coordenação de Aperfeiçoamento de Pessoal de Nível Superior (in particular through program CAPES-COFECUB 0899/2018). Research at IIP-UFRN is supported by Ministério da Educação and Ministério da Ciência, Tecnologia e Inovação.

APPENDIX A: BOSONIZATION FORMULAS

In this Appendix, we write down the bosonized expressions for some important quantities in the interacting case.

After the gauge transformation $\psi_\ell \to e^{-i\mu_\ell t}\psi_\ell$, the Kondo Hamiltonian in Eq. (47) and the current operator defined in Eq. (22) are given by

$$H_K^{\rm int}(t) = \pi v_F \lambda_K \big[S_0^+ F(t) + S_0^- F^\dagger(t) + S_0^z G(t)\big], \tag{A1}$$

$$\hat{j}(t) = ie\pi v_F \Gamma_K \big[S_0^+ f(t) - S_0^- f^\dagger(t) + S_0^z g(t)\big], \tag{A2}$$

where

$$f(t) = \frac{-i}{\pi\alpha} e^{-i\sqrt{\pi}\phi_s^+(0)} \sin[eVt + \sqrt{\pi}\phi_c^-(0)], \tag{A3}$$

$$g(t) = \frac{-2i}{\pi\alpha} \sin[\sqrt{\pi}\phi_s^-(0)] \cos[eVt + \sqrt{\pi}\phi_c^-(0)], \tag{A4}$$

$$F(t) = \frac{1}{2\pi\alpha} e^{-i\sqrt{\pi}\phi_s^+(0)} \{\cos[\sqrt{\pi}\phi_s^-(0)] + \mathcal{C}\cos[\sqrt{\pi}\phi_c^-(0) + eVt]\}, \tag{A5}$$

$$G(t) = -\frac{1}{\sqrt{4\pi}}\partial_x\phi_s^+(0) - \frac{\mathcal{C}}{\pi\alpha}\sin[\sqrt{\pi}\phi_c^-(0) + eVt]\sin[\sqrt{\pi}\phi_s^-(0)], \tag{A6}$$

where $\phi_\lambda^\pm(x)$ are defined in Eq. (52) and $\lambda_K\mathcal{C} \equiv \Gamma_K$. For a noninteracting system, we have $\lambda_K = \Gamma_K$, consequently $\mathcal{C} = 1$. In the above expressions we do not explicitly write the Klein factors, but they must be taken into account when calculating the correlators.

APPENDIX B: THREE-POINT FUNCTION

In this Appendix, we present some details on the calculation of the third-order correlator in Eq. (51). The charge part of the correlator reduces to a two-point function as given in Eq. (50). The spin part is equivalent to the bosonization of the fermion operators in

$$C \equiv \langle T\psi_\downarrow^\dagger(t)\psi_\uparrow(t)\psi_\uparrow^\dagger(t')\psi_\downarrow(t') \times [:\psi_\uparrow^\dagger(t'')\psi_\uparrow(t'') - \psi_\downarrow^\dagger(t'')\psi_\downarrow(t''):]\rangle. \tag{B1}$$

For a noninteracting system, we can calculate this correlator by applying Wick's theorem. Using the Green's function $\langle T\psi_\sigma^\dagger(t)\psi_\sigma(t')\rangle = \frac{-i}{2\pi v_F}\frac{1}{t-t'}$, we obtain the result for $t > t' > t''$:

$$C = -\frac{2i}{(2\pi v_F)^3}\frac{1}{(t-t')(t-t'')(t'-t'')}. \tag{B2}$$

We can now calculate the same correlator using the bosonization dictionary. For a system with open boundary conditions, we use $\psi_\sigma(t) = \frac{F_\sigma}{\sqrt{2\pi\alpha}} e^{-i\sqrt{\pi}\phi_\sigma(t)}$ and $:\psi_\sigma^\dagger(t)\psi_\sigma(t): = -\frac{1}{\sqrt{4\pi}}\partial_x\phi_\sigma(t)$ for a chiral boson that obeys $[\phi_\sigma(x), \phi_{\sigma'}(x')] = i\pi\delta_{\sigma\sigma'}\mathrm{sgn}(x-x')$. The correlator in Eq. (B1) becomes

$$C = -\frac{\langle T e^{-i\sqrt{2\pi}\phi_s(t)} e^{i\sqrt{2\pi}\phi_s(t')}\partial_x\phi_s(t'')\rangle}{(2\pi\alpha)^2\sqrt{2\pi}}. \tag{B3}$$

Using Wick's theorem for free bosons, we obtain

$$\begin{aligned} C &= -\frac{i}{(2\pi\alpha)^2}\langle T e^{-i\sqrt{2\pi}\phi_s(t)} e^{i\sqrt{2\pi}\phi_s(t')}\rangle \\ &\quad\times [\langle T\phi_s(t')\partial_x\phi_s(t'')\rangle - \langle T\phi_s(t)\partial_x\phi_s(t'')\rangle] \\ &= -\frac{i}{(2\pi\alpha)^2}\frac{1}{[1+i\Lambda(t-t')]^2} \\ &\quad\times\left[\frac{-i/\pi\alpha}{1+i\Lambda(t'-t'')} - \frac{-i/\pi\alpha}{1+i\Lambda(t-t'')}\right] \\ &\overset{\alpha\to 0}{=} -\frac{2i}{(2\pi v_F)^3}\frac{1}{(t-t')(t-t'')(t'-t'')}, \end{aligned} \tag{B4}$$

for $t > t' > t''$ and $K_s = 1$. Thus, the result of the bosonic calculation in Eq. (B4) is consistent with the fermionic one in Eq. (B2).

[1] I. Affleck, in *Exact Methods in Low-Dimensional Statistical Physics and Quantum Computing*, edited by J. Jacobsen, S. Ouvry, V. Pasquier, and D. S. L. Cugliandolo (Oxford University Press, Oxford, 2010).

[2] P.B. Vigman, Pis'ma Zh. Eksp. Teor. Fiz. **31**, 392 (1980).

[3] N. Andrei, K. Furuya, and J. H. Lowenstein, Rev. Mod. Phys. **55**, 331 (1983).

[4] J. L. Cardy, Nucl. Phys. B **240**, 514 (1984).

[5] I. Affleck and A. W. Ludwig, Nucl. Phys. B **360**, 641 (1991).

[6] R. Bulla, T. A. Costi, and T. Pruschke, Rev. Mod. Phys. **80**, 395 (2008).

[7] S. R. White, Phys. Rev. Lett. **69**, 2863 (1992).

[8] D. Goldhaber-Gordon, H. Shtrikman, D. Mahalu, D. Abusch-Magder, U. Meirav, and M. A. Kastner, Nature (London) **391**, 156 (1998).

[9] S. M. Cronenwett, T. H. Oosterkamp, and L. P. Kouwenhoven, Science **281**, 540 (1998).

[10] J. Bauer, C. Salomon, and E. Demler, Phys. Rev. Lett. **111**, 215304 (2013).

[11] Y. Nishida, Phys. Rev. Lett. **111**, 135301 (2013).

[12] L. Riegger, N. Darkwah Oppong, M. Höfer, D. R. Fernandes, I. Bloch, and S. Fölling, Phys. Rev. Lett. **120**, 143601 (2018).

[13] M. Kanász-Nagy, Y. Ashida, T. Shi, C. P. Moca, T. N. Ikeda, S. Fölling, J. I. Cirac, G. Zaránd, and E. A. Demler, Phys. Rev. B **97**, 155156 (2018).

[14] J. Eisert, M. Friesdorf, and C. Gogolin, Nat. Phys. **11**, 124 (2015).

[15] A. Mitra, Annu. Rev. Condens. Matter Phys. **9**, 245 (2018).

[16] P. Calabrese and J. Cardy, Phys. Rev. Lett. **96**, 136801 (2006).

[17] M. A. Cazalilla, Phys. Rev. Lett. **97**, 156403 (2006).

[18] P. Calabrese and J. Cardy, J. Stat. Mech. (2016) 064003.

[19] A. Hewson, *The Kondo Problem to Heavy Fermions*, Cambridge Studies in Magnetism (Cambridge University Press, Cambridge, 1997).

[20] P. Nozières, J. Low Temp. Phys. **17**, 31 (1974).

[21] V. Barzykin and I. Affleck, Phys. Rev. Lett. **76**, 4959 (1996).
[22] P. Simon and I. Affleck, Phys. Rev. B **64**, 085308 (2001).
[23] P. Simon and I. Affleck, Phys. Rev. B **68**, 115304 (2003).
[24] L. Borda, Phys. Rev. B **75**, 041307(R) (2007).
[25] R. G. Pereira, N. Laflorencie, I. Affleck, and B. I. Halperin, Phys. Rev. B **77**, 125327 (2008).
[26] I. Affleck, The Kondo screening cloud what it is and how to observe it, in *Perspectives of Mesoscopic Physics - Dedicated to Yoseph Imry's 70th Birthday*, pp. 1-44 (World Scientific, 2010).
[27] I. V. Borzenets, J. Shim, J. C. H. Chen, A. Ludwig, A. D. Wieck, S. Tarucha, H. S. Sim, and M. Yamamoto, Nature (London) **579**, 210 (2020).
[28] P. Nordlander, M. Pustilnik, Y. Meir, N. S. Wingreen, and D. C. Langreth, Phys. Rev. Lett. **83**, 808 (1999).
[29] F. B. Anders and A. Schiller, Phys. Rev. Lett. **95**, 196801 (2005).
[30] S. Kehrein, Phys. Rev. Lett. **95**, 056602 (2005).
[31] D. Lobaskin and S. Kehrein, Phys. Rev. B **71**, 193303 (2005).
[32] A. Hackl, D. Roosen, S. Kehrein, and W. Hofstetter, Phys. Rev. Lett. **102**, 196601 (2009).
[33] M. Pletyukhov, D. Schuricht, and H. Schoeller, Phys. Rev. Lett. **104**, 106801 (2010).
[34] M. Pletyukhov and H. Schoeller, Phys. Rev. Lett. **108**, 260601 (2012).
[35] S. Andergassen, M. Pletyukhov, D. Schuricht, H. Schoeller, and L. Borda, Phys. Rev. B **83**, 205103 (2011).
[36] M. Medvedyeva, A. Hoffmann, and S. Kehrein, Phys. Rev. B **88**, 094306 (2013).
[37] R. Vasseur, K. Trinh, S. Haas, and H. Saleur, Phys. Rev. Lett. **110**, 240601 (2013).
[38] B. Lechtenberg and F. B. Anders, Phys. Rev. B **90**, 045117 (2014).
[39] D. M. Kennes, V. Meden, and R. Vasseur, Phys. Rev. B **90**, 115101 (2014).
[40] M. Nuss, M. Ganahl, E. Arrigoni, W. von der Linden, and H. G. Evertz, Phys. Rev. B **91**, 085127 (2015).
[41] S. Ghosh, P. Ribeiro, and M. Haque, J. Stat. Mech.: Theory Exp. (2015) P08002.
[42] A. E. Antipov, Q. Dong, and E. Gull, Phys. Rev. Lett. **116**, 036801 (2016).
[43] H. T. M. Nghiem and T. A. Costi, Phys. Rev. Lett. **119**, 156601 (2017).
[44] I. Krivenko, J. Kleinhenz, G. Cohen, and E. Gull, Phys. Rev. B **100**, 201104(R) (2019).
[45] S. Goto and I. Danshita, Phys. Rev. Lett. **123**, 143002 (2019).
[46] M. Schiró and A. Mitra, Phys. Rev. B **91**, 235126 (2015).
[47] M. Pustilnik and L. Glazman, J. Phys.: Condens. Matter **16**, R513 (2004).
[48] H. Bragança, M. F. Cavalcante, R. G. Pereira, and M. C. O. Aguiar, Phys. Rev. B **103**, 125152 (2021).
[49] M. Fabrizio and A. O. Gogolin, Phys. Rev. B **51**, 17827 (1995).
[50] G. Stefanucci and R. van Leeuwen, *Nonequilibrium Many-Body Theory of Quantum Systems: A Modern Introduction* (Cambridge University Press, Cambridge, 2013).
[51] T. Giamarchi, *Quantum Physics in One Dimension* (Clarendon Press, Oxford, 2003).
[52] A. Gogolin, A. Nersesyan, and A. Tsvelik, *Bosonization and Strongly Correlated Systems* (Cambridge University Press, Cambridge, 2004).
[53] F. D. M. Haldane, J. Phys. C **14**, 2585 (1981).
[54] D.-H. Lee and J. Toner, Phys. Rev. Lett. **69**, 3378 (1992).
[55] A. Furusaki and N. Nagaosa, Phys. Rev. Lett. **72**, 892 (1994).
[56] P. Fröjdh and H. Johannesson, Phys. Rev. Lett. **75**, 300 (1995).
[57] S. Eggert and I. Affleck, Phys. Rev. B **46**, 10866 (1992).
[58] N. Laflorencie, E. S. Sorensen, and I. Affleck, J. Stat. Mech. (2008) P02007.
[59] D. Giuliano, P. Sodano, and A. Trombettoni, Phys. Rev. A **96**, 033603 (2017).